Reflection of solar wind protons on the Martian bow shock: Investigations by means of 3-dimensional simulations

Emilie Richer, Gérard Chanteur, Ronan Modolo, Eduard Dubinin

Reflection of solar wind protons on the Martian bow shock: Investigations by means of 3-dimensional simulations

E. Richer,[1] G. M. Chanteur,[1] R. Modolo,[2] and E. Dubinin[3]

Received 22 June 2012; revised 26 July 2012; accepted 26 July 2012; published 1 September 2012.

[1] The reflection of solar wind protons on the Martian bow shock (BS) is investigated by means of three-dimensional simulation models. A two steps approach is adopted to allow a detailed analysis of the reflected population. Firstly, the 3-dimensional hybrid model of Modolo et al. (2005) is used to compute a stationary state of the interaction of the solar wind (SW) with Mars. Secondly, the motion of test particles is followed in the electromagnetic field computed by the hybrid simulation meanwhile detection criteria defined to identify reflected protons are applied. This study demonstrates some effects of the large curvature of a planetary BS on the structure of the foreshock. Reflected protons encounter the BS in a region encompassing parts of the quasi-perpendicular and quasi-parallel shocks, and exit the shock mainly from the quasi-parallel region. The energy spectrum of all reflected protons extends from 0 to almost 15keV. A virtual omnidirectional detector (VOD) is used to compute the local omnidirectional flux of reflected protons at various locations upstream of the BS. Spatial variations of this omnidirectional flux indicate the location and spatial extent of the proton foreshock and demonstrate its shift, increasing with the distance downstream, in the direction opposite to the motional electric field of the SW. Local energy spectra computed from the VOD observations demonstrate the existence of an energy gradient along the direction of the convection electric field.
Citation: Richer, E., G. M. Chanteur, R. Modolo, and E. Dubinin (2012), Reflection of solar wind protons on the Martian bow shock: Investigations by means of 3-dimensional simulations, *Geophys. Res. Lett.*, *39*, L17101, doi:10.1029/2012GL052858.

1. Introduction

[2] The reflection of part of the ions incident on a planetary BS is quite common in the Solar System and is one of the main dissipation mechanisms for supercritical collisionless shocks in space plasmas. The first identification of SW ions reflected at the terrestrial BS has been presented by *Asbridge et al.* [1968]. Numerous following observations demonstrated the properties of this reflected population mainly composed of protons and a few percent of alpha particles [*Paschmann et al.*, 1981; *Ipavich et al.*, 1981]. The majority of current knowledge on these reflected ions comes from terrestrial observation on foreshock ions. They are categorized in two main populations: beam-like population at limited energy range of several keV, and diffuse population at wide energy range with spectra indicative of Fermi acceleration: see *Eastwood et al.* [2005] for a recent and exhaustive review. Simulation studies have also contributed to elucidate the reflection of particles on shocks. *Burgess* [1987] presented the first simulation study of oblique shocks, with a one-dimensional hybrid code and test particle calculations, which demonstrated *inter alia* that the reflection rate of SW protons is correlated with the shock normal angle.

[3] Up to now the effect of the curvature of a BS on the reflection of incident particles has drawn little attention as it was not a pertinent factor in the most investigated cases. Nevertheless the question arises when considering terrestrial planets with small obstacle size such as Mars [*Yamauchi et al.*, 2011] and Mercury. For typical SW conditions, e.g. 1keV energy for protons, the radius of curvature of the BS at the subsolar point is comparable to the Larmor radius for Mars and to some extent for Mercury. Therefore, neither the Martian nor the Hermean BS can be considered as plane shocks when considering the reflection of solar wind ions. The first evidence of ions reflected on the Martian BS was provided by the ASPERA instrument on-board the Phobos-2 spacecraft [*Dubinin et al.*, 1993] but the available information about this reflected population remained rather scarce until recently when further properties have been revealed by a detailed analysis of Mars-Express observations [*Yamauchi et al.*, 2011].

[4] We present a genuinely 3-dimensional simulation study which provides new information on SW protons reflected on the Martian BS , especially in order to set back *in situ* observations in a global context or to make predictions for future observations. The following sections expose the methodology including the simulation process and the identification criteria of reflected particles, then the main results, and the conclusions.

2. Methodology

[5] First, a stationary state of the interaction between Mars and the SW is computed by running the three-dimensional hybrid simulation model of *Modolo et al.* [2005]. The stationary self-consistent electromagnetic field is sampled and recorded nine times, every two cyclotron periods of protons in the SW. These nine snapshots of the electromagnetic field in the simulation domain differ only by spatial fluctuations ; they are used to run successively nine test particle simulations tracking SW protons in the simulation domain in order to estimate statistics of the results. Reflected protons are of course present in the self-consistent hybrid simulation

[1]Laboratoire de Physique des Plasmas, Ecole Polytechnique, Palaiseau, France.
[2]LATMOS, UVSQ IPSL, Guyancourt, France.
[3]MPS, Katlenburg-Lindau, Germany.

Corresponding author: E. Richer, Laboratoire de Physique des Plasmas, Ecole Polytechnique, Route de Saclay, FR-91128 Palaiseau, France. (emilie.richer@lpp.polytechnique.fr)

0094-8276/12/2012GL052858

nevertheless their identification is difficult : simple criteria based upon the energy of the particles or on the direction of their motion fail to detect a large fraction of reflected particles. The adopted two steps approach is the simplest and may be the best way to detect all reflected particles. Another advantage of the two steps approach is the possibility to follow an arbitrary large number of test particles in order to improve statistics. A similar method has been used to study the capture of alpha particles by the Martian atmosphere [*Chanteur et al.*, 2009].

2.1. Hybrid Simulation

[6] In the hybrid framework, a kinetic description is used for ions while electrons are assumed to be an inertialess fluid ensuring the neutrality of the plasma and contributing to current and pressure. The hybrid simulation model is run on a uniform cartesian mesh with a spatial resolution of 300 km. The reference frame is the Mars Solar Orbital frame (MSO), a direct orthogonal frame defined by the X axis pointing toward Sun, and the Y axis antiparallel to Mars orbital velocity. The solar wind velocity is antiparallel to the X axis and the IMF vector is in the xOz plane with a positive Z component. The computational domain has the following bounds : $-6R_M \leq X \leq +3R_M$ and $-11R_M \leq Y, Z \leq +11R_M$. Typical parameters of the solar wind plasma at the Martian orbit are used : the IMF vector is equal to (−1.3, 0., 2.1)nT, the solar wind has a particle density of 1.3 cm^{-3} including 5% of He^{++}, SW ions have Maxwellian distributions with temperatures equal to 9 eV for protons and 36 eV for alpha particles, the electronic temperature is equal to 16 eV, and the SW speed is set to 500 km s^{-1}. These parameters lead to a plasma beta equal to 2.4 and an Alfvén Mach number equal to 10.5. Such SW parameters are representative of observational values [*Fränz et al.*, 2006]. The computed BS is in good agreement with the MGS and Phobos-2 observations [*Modolo et al.*,2005], it contains quasi-parallel and quasi-perpendicular shock regions, and exhibits asymmetries along both Z and Y directions as well as a realistic three-dimensional curvature. In *Modolo et al.* [2005], planetary ions are produced through ionisation of the exosphere either by solar photons, electronic impacts or charge exchanges. Details concerning the chosen neutral environment, as well as the implementation of the ionization mechanisms, are given in *Modolo et al.* [2005, 2006]. As shown by *Modolo et al.* [2006] both the position and the shape of the Martian BS are weakly sensitive to the solar activity, hence the conditions of solar maximum used in the hybrid simulation are not expected to play a major role in the present study. *Mazelle et al.* [2004] have discussed the structure of the Martian BS: its thickness is comparable to the convective gyroradius of SW protons in the quasi-perpendicular region, except in the vicinity of the subsolar point where it is smaller. Structures of the BS at scales smaller than the spatial resolution of the simulation (Δx = 300 km) are not resolved.

2.2. Test-Particle Simulations

[7] Test-particles are injected through the entry face of the simulation box (X = $3R_M$) with the velocity distribution function of SW protons used in the hybrid simulation. Trajectories of test particles are computed sequentially, one after the other, from the entry point of the particle to its exit point usually through a face of the simulation domain, or exceptionally into the atmosphere of the planet. Each trajectory is analyzed immediately after completion of its computation by using temporarily stored information along the path of the particle. The magnetic field acting on particle j at position $(\vec{x}_j(t_n))$ is recorded as $\vec{B}_j(t_n)$ and used to identify crossings of the BS. Upstream of the BS the magnetic induction is equal to the imposed IMF except for fluctuations inherent to the hybrid scheme: thus the upstream SW region is defined as the region where the magnetic field does not spread too much from the imposed nominal IMF. As long as $\Delta B_j^2(t_n) = \left(\vec{B}_j(t_n) - \vec{B}_{IMF}\right)^2$ is smaller than a given threshold ΔB_0^2, chosen larger than the mean square fluctuations of the magnetic field upstream of the BS and here equal to 5% of the square of the IMF, the particle is considered upstream of the BS. The first time step when $\Delta B_j^2 > \Delta B_0^2$ indicates the first inward BS crossing and the last time step when this condition is fulfilled corresponds to the last outward BS crossing.

[8] Most of SW protons which encounter the BS pass through it and exit the simulation domain in the Martian wake downstream of the shock meanwhile a small fraction leaves the simulation domain upstream of the shock. A particle having encountered the BS and leaving the simulation domain in the upstream region is potentially a reflected proton. In order to discriminate between reflected protons and protons with trajectories almost tangential to the BS which cross repeatedly the BS when moving successively into and out of the magnetosheath due to their gyrating motion, a second criterion is used. A particle is identified as reflected if its last outward BS crossing occurs upstream of a given abscissa X_0 chosen equal to −5.3 R_M (*i.e.* 0.7 R_M upstream of the exit plane). This supplementary criterion allows to define the global reflection rate over a well delimited portion of the BS upstream of a given abscissa.

3. Results

[9] Each of the nine test particle simulations tracks 10^6 test-particles, about 6×10^5 of those particles hit the BS upstream of the plane of constant abscissa $X_0 = -5.3R_M$, and among them between 6 to 7×10^4 particles are reflected giving a global reflection rate of solar wind protons of the order of 10 to 12% on the part of the BS located upstream of $X_0 = -5.3R_M$. The energy spectrum of all these reflected protons extends from 0 to almost 15keV. In order to mimic *in situ* measurements by spacecraft we compute local omnidirectional fluxes and energy spectra of reflected protons detected by virtual omnidirectional detectors (VODs) at various locations. A VOD is a sphere with a given radius (usually a fraction of R_M) which counts each test particle crossing its surface, without affecting its trajectory, and records its energy. The number of counts recorded by a VOD grows linearly with the geometrical area of the VOD as long as the VOD covers a uniform region: a VOD radius equal to $0.5R_M$ is the best compromise to get significant statistics when considering spatial gradients in the simulated foreshock. Number of counts are converted into fluxes by taking into account the size of the VOD and the statistical weight of the test particles.

3.1. Where Are Solar Wind Protons Reflected?

[10] For each reflected test particle we know from the analysis of its trajectory the locations of its entry and of its

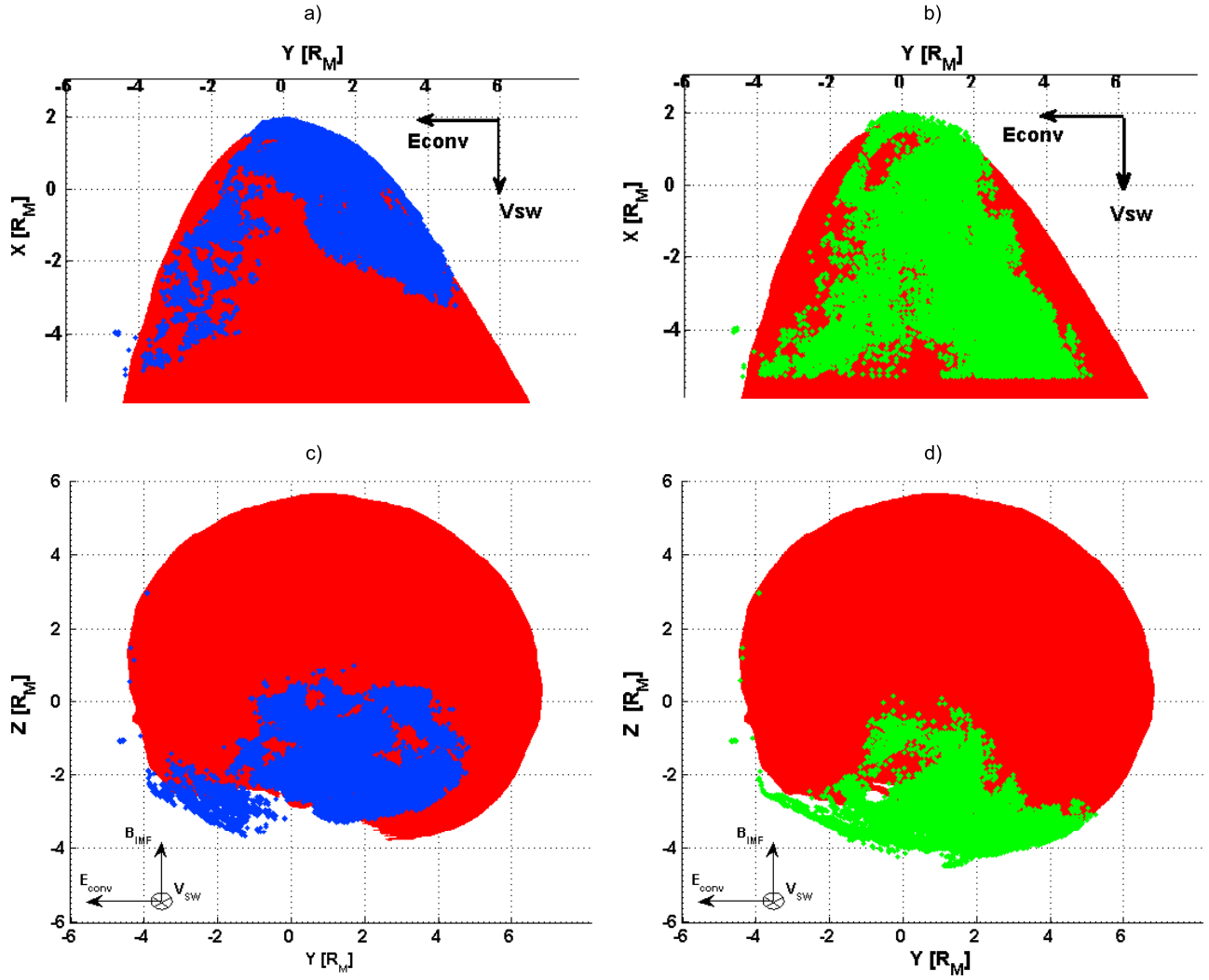

Figure 1. (a and b) XY_{MSO} and (c and d) YZ_{MSO} projections of an isovalue surface of the magnetic field representing the simulated Martian BS. Clouds of entry (blue) and exit (green) points of the reflected protons are overlaid separately on the different projections of the BS, respectively on the left and right columns of the figure. The quasi-parallel shock region corresponds to the "hole" in the surface glimpsed in Figures 1c and 1d in the negative Z_{MSO} region. Projections of the SW direction, motional electric field and IMF are indicated in the different planes.

exit from the BS. Figures 1(a and c) and Figures 1(b and d) illustrate respectively the locations of the first and last encounters of the reflected SW protons with the BS for one of the nine test particle simulations. Reflected protons encounter the BS mostly in the quasi-perpendicular region with a broad distribution of θ_{Bn}, the oriented angle from the IMF vector to the local normal to the BS pointing upstream, between 0.60π and 0.85π while they leave the BS mainly in the quasi-parallel region with a relatively narrow distribution of θ_{Bn} extending between 0.80π and 0.95π at half the maximum height of the distribution function. Both clouds of points are located on the same side of the BS with $Z_{MSO} < 0$ but the cloud of exit points is shifted toward the region of parallel shock. These facts are common to the nine test particle simulations done.

3.2. The Proton Foreshock

[11] A coarse sampling by VODs of a few planes parallel to MSO coordinates planes creates maps of the omnidirectional (OD) flux of reflected protons detected locally; indeed the OD flux is normalized to the nominal flux of SW protons. This provides a sketch of the Martian proton foreshock. Figures 2a and 2b illustrate this sampling respectively in the two planes $Y_{MSO} = 0R_M$ and $X_{MSO} = -3R_M$. Maps in the upper row display the normalized OD flux averaged over the nine test particle simulations meanwhile the lower row shows maps of the variances in the respective planes. These maps demonstrate that the proton foreshock extends far downstream of Mars below the parallel shock and that it is shifted with respect to the Sun-Mars line in the direction opposite to the convection electric field. This shift increases further downstream in the wake. The thickness of the mean foreshock along the Y_{MSO} direction is of the order of $4R_M$ (Figure 2b) leading to a potential drop equal to 14kV across the foreshock. Although stationary the simulated BS is affected by fluctuations which partly explain the observed variance of the results, the other factor being the limited statistics at low fluxes. The Martian proton foreshock thus appears as a thick wing attached to the

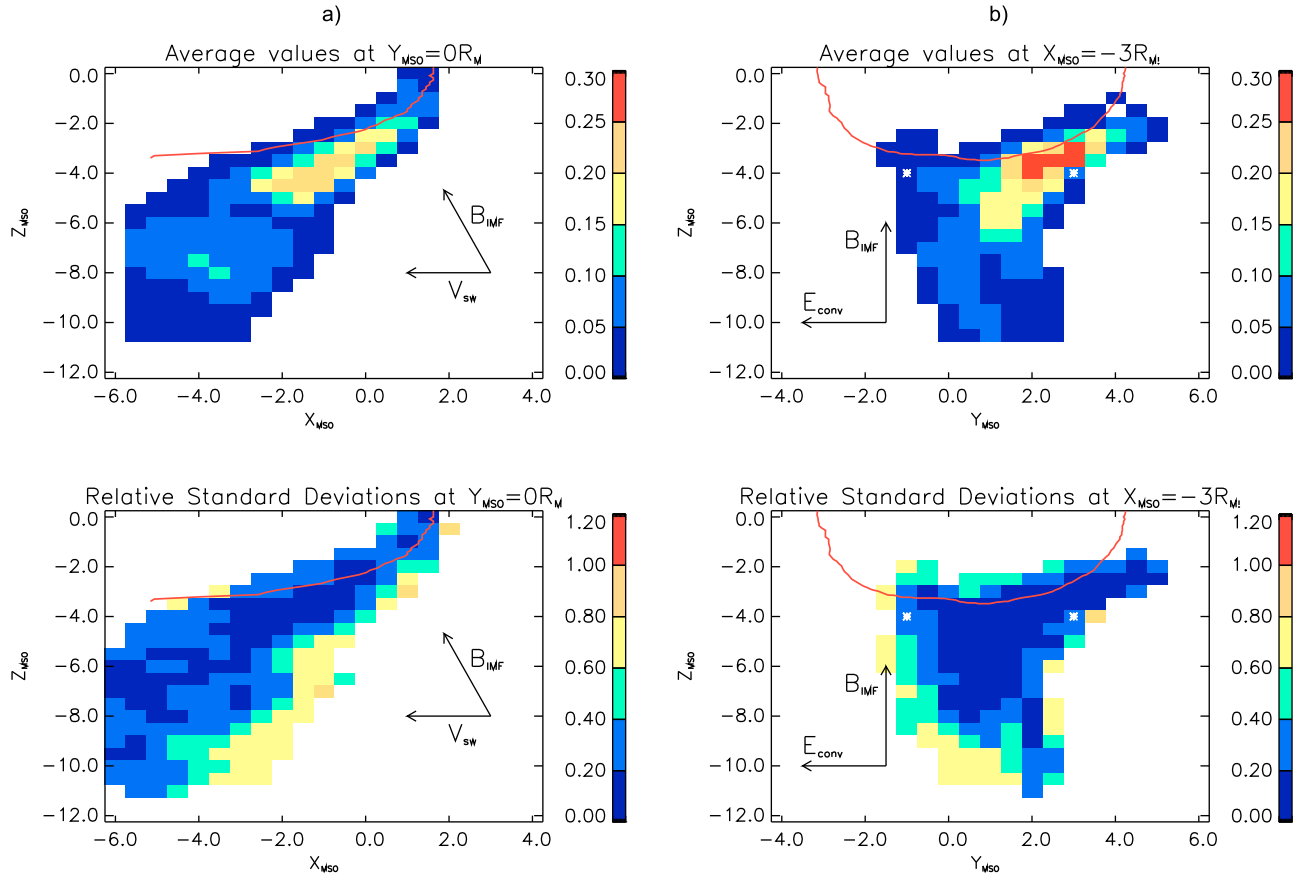

Figure 2. (a) Normalized omnidirectional flux of reflected SW protons in two plane cuts: results for the XOZ plane containing the center of the planet (Y_{MSO} = 0) and (b) results for the plane parallel to the terminator and downstream of it at X_{MSO} = −3R_M. Top panels show the average values computed over the nine test-particle simulations corresponding to different snapshots of the self-consistent em field of the hybrid simulation, while bottom panels present the relative standard deviations. The red line in the respective planes indicates the BS location determined by a sudden jump of density by more than a factor two. White stars in Figure 3b indicate the position of the two VODs used to compute local spectra displayed in Figure 3.

parallel region of the BS and oblique with respect to the SW bulk flow. The normalized OD flux of reflected SW protons reaches a maximum equal to 0.25 around $(X,Y,Z)_{MSO}$ = (−1., 0., −4.)R_M.

[12] During their trajectory, reflected SW protons can explore the magnetosheath region, up to about 1–1.5 Martian radius downstream of the BS, before leaving the simulation domain in the "undisturbed" SW region (Figure 2). This behavior is indicative of the large gyroradii of these particles.

3.3. Energy Range of the Reflected Solar Wind Protons

[13] Figure 3 shows the local energy spectra at the edges of the foreshock along the Y_{MSO} direction at X = −3 R_M and Z = −4 R_M. These spectra are averaged over the nine test particle simulations done and the error bars indicate levels at ± one standard deviation. The upper panel corresponds to the edge where the convection electric field is pointing outward of the foreshock, a location where some detected particles have been accelerated by the electric field across a large fraction of the thickness of the foreshock. This explains both the depletion of the OD flux below 3keV and the energetic tail extending up to 15keV. The high energy tail of the local energy spectrum extends to almost 15keV in good agreement with the maximum acceleration achievable through the foreshock. The situation on the opposite edge, where the convection electric field is pointing toward the foreshock, is illustrated by the lower panel with a spectrum extending from 0 to 5.5keV. Protons observed on this side have mainly been decelerated by the motional electric field which explains their almost monotonously decreasing spectrum.

4. Conclusions

[14] The large curvature of the Martian BS around its subsolar point has observable consequences on the proton foreshock. By contrast to situations known at Venus and Earth there are no reflected protons upstream of the nose of the Martian BS: the proton foreshock lies entirely downstream of the subsolar point of the BS, looks like a thick wing mainly attached to the parallel shock, and has a width of 4R_M along the direction of the convection electric field which is of the same order as the diameter of the gyromotion of most reflected protons. *Yamauchi et al.* [2011] have reported a

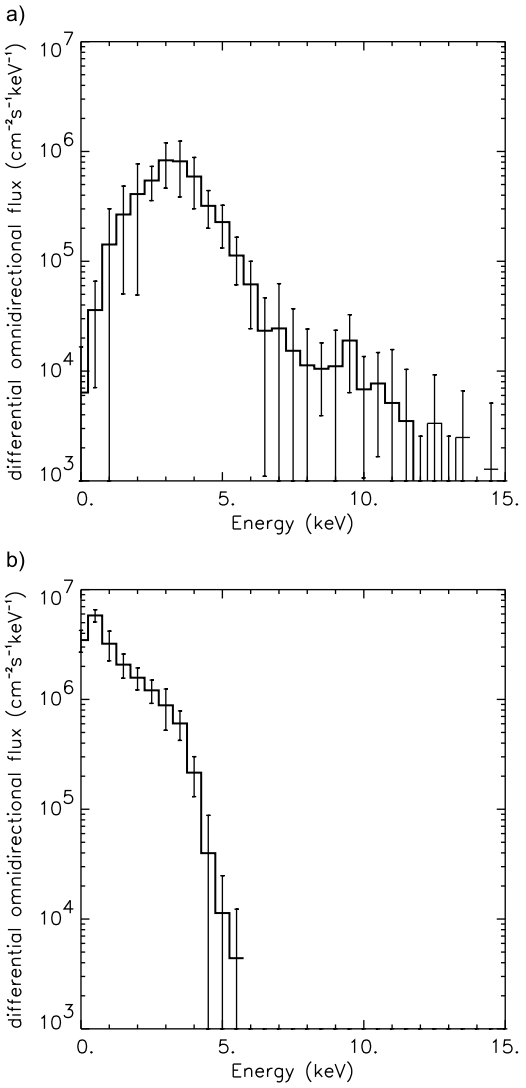

Figure 3. (a and b) Averaged energy spectra of reflected SW protons detected by VODs centered downstream of Mars at $(X, Y, Z)_{MSO} = (-3., -1., -4.5)\ R_M$ and $(-3., 3, -4.5)\ R_M$ respectively, *i.e.*at the edges of the foreshock along the Y_{MSO} direction. The energy resolution is equal to 0.5keV and error bars, corresponding to plus/minus one standard deviation, are plotted for each energy channel. In Figure 3a, corresponding to the edge where the SW convection electric field is pointing outward of the foreshock, the energy range extends from 0 to almost 15keV and the differential OD flux reaches a maximum slightly above 3keV. On the opposite edge, where the SW convection electric field is pointing inward the foreshock, the energy spectrum displayed in Figure 3b extends from 0 to 5.5keV only and is decreasing monotonically above 250 keV.

tailward skew of reflected particles which is in agreement with the present simulation findings. The observed proton foreshock is shifted in the direction opposite to the motional electric field of the SW and this shift increases as reflected protons move downstream. Local energy spectra depend upon the position of the observation point inside the foreshock: spectra show more energetic reflected particles on the edge of the foreshock where the convection electric field is pointing outward of the foreshock meanwhile spectra on the opposite side present an upper cutoff at a much lower energy. Investigations of pickup protons and solar wind alpha particles reflected on the Martian BS are under progress and will be published later. Similar effects are expected at Mercury due to the large curvature of its BS around the subsolar point.

[15] **Acknowledgments.** The authors acknowledge a financial support of their activity by Programme Soleil Heliosphère Magnétosphère of the French space agency CNES. Research at LATMOS have been partly supported by ANR-CNRS through contract ANR-09-BLAN-223. E.R.'s PhD is funded by University Pierre and Marie Curie in Paris (UPMC, ED389).

[16] The Editor thanks two anonymous reviewers for their assistance in evaluating this paper.

References

Asbridge, J. R., S. J. Bame, and I. B. Strong (1968), Outward flow of protons from the Earth's bow shock, *J. Geophys. Res.*, *73*, 5777–5782, doi:10.1029/JA073i017p05777.

Burgess, D. (1987), Shock drift acceleration at low energies, *J. Geophys. Res.*, *92*, 1119–1130, doi:10.1029/JA092iA02p01119.

Chanteur, G. M., E. Dubinin, R. Modolo, and M. Fraenz (2009), Capture of solar wind alpha-particles by the Martian atmosphere, *Geophys. Res. Lett.*, *36*, L23105, doi:10.1029/2009GL040235.

Dubinin, E., R. Lundin, H. Koskinen, and O. Norberg (1993), Cold ions at the Martian bow shock: PHOBOS observations, *J. Geophys. Res.*, *98*, 5617–5623, doi:10.1029/92JA02374.

Eastwood, J. P., E. A. Lucek, C. Mazelle, K. Meziane, Y. Narita, J. Pickett, and R. A. Treumann (2005), The foreshock, *Space Sci. Rev.*, *118*, 41–94, doi:10.1007/s11214-005-3824-3.

Fränz, M., et al. (2006), Plasma moments in the environment of Mars. Mars Express ASPERA-3 observations, *Space Sci. Rev.*, *126*, 165–207, doi:10.1007/s11214-006-9115-9.

Ipavich, F. M., A. B. Galvin, G. Gloeckler, M. Scholer, and D. Hovestadt (1981), A statistical survey of ions observed upstream of the Earth's bow shock: Energy spectra, composition, and spatial variation, *J. Geophys. Res.*, *86*, 4337–4342, doi:10.1029/JA086iA06p04337.

Mazelle, C., et al. (2004), Bow shock and upstream phenomena at Mars, *Space Sci. Rev.*, *111*, 115–181.

Modolo, R., G. M. Chanteur, E. Dubinin, and A. P. Matthews (2005), Influence of the solar euv flux on the Martian plasma environment, *Ann. Geophys.*, *23*(2), 433–444, doi:10.5194/angeo-23-433-2005.

Modolo, R., G. M. Chanteur, E. Dubinin, and A. P. Matthews (2006), Simulated solar wind plasma interaction with the Martian exosphere: Influence of the solar EUV flux on the bow shock and the magnetic pile-up boundary, *Ann. Geophys.*, *24*, 3403–3410, doi:10.5194/angeo-24-3403-2006.

Paschmann, G., N. Sckopke, I. Papamastorakis, J. R. Asbridge, S. J. Bame, and J. T. Gosling (1981), Characteristics of reflected and diffuse ions upstream from the Earth's bow shock, *J. Geophys. Res.*, *86*, 4355–4364, doi:10.1029/JA086iA06p04355.

Yamauchi, M., et al. (2011), Comparison of accelerated ion populations observed upstream of the bow shocks at Venus and Mars, *Ann. Geophys.*, *29*, 511–528, doi:10.5194/angeo-29-511-2011.